Hyperfine-structure quantum beats: application of the graphical methods of angular-momentum theory to the calculation of intensity profiles

J. Phys. B: Atom. Molec. Phys., Vol. 10, No. 18, 1977. Printed in Great Britain.

Hyperfine-structure quantum beats: application of the graphical methods of angular-momentum theory to the calculation of intensity profiles

R Luypaert† and J Van Craen‡
Departement Natuurkunde, Vrije Universiteit Brussel, Belgium

Received 25 April 1977, in final form 4 July 1977

Abstract. A theoretical study of quantum-beat intensity profiles is presented for the case of zero-field hyperfine-structure beats. By means of the graphical methods of angular-momentum theory, an explicit expression for the quantum-beat profiles, in the form of a multipole expansion, is obtained.

1. Introduction

Among the techniques of high-resolution spectroscopy those in which the atomic system under study is excited into a coherent superposition of states with nearly equal energy have found new applications in recent years. The evolution of the coherence, monitored by its effect on the polarisation of the fluorescent light, provides a means of obtaining spectroscopic information about the excited states.

Well established examples of this kind of technique are the Hanle effect (Hanle 1924), level-crossing (Colegrove *et al* 1959) and modulated-pumping experiments (Aleksandrov 1963, Corney and Series 1964). Another atomic coherence phenomenon is the quantum-beat effect, in which the atoms are brought into a coherent superposition of excited states by the use of a short pulse. Under suitable conditions the coherence shows up as modulation of the exponentially decaying fluorescent light intensity at the Bohr frequencies corresponding to the excited-state energy splittings. In spite of its greater conceptual simplicity this effect has not until recently been used as a comparable spectroscopic tool. Being a transient effect it can only be observed if sufficiently 'fast' excitation and detection are available and for a long time that was not the case.

Quantum-beat studies were first carried out for Zeeman structures by Dodd *et al* (1964) and Aleksandrov (1964) using continuously emitting spectral lamps shuttered by Kerr cells. The obvious drawbacks of this kind of excitation (rather long pulses of weak intensity) were overcome by the introduction of various other excitation methods such as electron bombardment (Hadeishi and Nierenberg 1965) and beam–foil excitation (Andrä 1970), which also brought fine and hyperfine structures within the reach of experiment. These methods, however, suffer from a lack of

† Previously at J J Thomson Physical Laboratory, University of Reading.
‡ Fellow of the National Foundation of Scientific Research, Belgium.

selectivity and it is only the recent advent of pulsed tunable dye lasers which has enabled the quantum-beat phenomenon to provide the basis for a useful spectroscopic technique (Haroche *et al* 1973, Deech *et al* 1975).

In this paper a theoretical study of the intensity profiles obtained in hyperfine-structure quantum-beat experiments is presented. Starting from a basic expression for the time dependence of the fluorescence intensity observed after exciting an ensemble of atoms with a short pulse of resonant light, use is made of the graphical methods of angular-momentum theory in order to eliminate all irrelevant quantum numbers. The final result corresponds to an expansion in multipoles and is presented in a form from which the fundamental properties of the quantum beats can easily be derived. The main content of the analysis is similar to that reported by Haroche (1976) for fine-structure quantum beats. The graphical approach adopted here has the advantage of being both simple and straightforward, providing direct insight into the angular-momentum coupling schemes. Even in complicated cases, it eliminates the need for extensive algebraic calculations in order to derive compact, easy-to-evaluate expressions for the fluorescence profiles.

2. Review of the fundamental quantum-beat theory

The basic scheme for a typical quantum-beat experiment is shown in figure 1. A short pulse of resonant light of polarisation $\boldsymbol{e}_e$ excites an ensemble of atoms from the initial states $\{|i\rangle\}$ to the excited states $\{|e\rangle\}$. The intensity of fluorescent light with polarisation $\boldsymbol{e}_d$, generated when the excited states decay to the final states $\{|f\rangle\}$, is then monitored as a function of time.

Theoretical expressions for the fluorescence intensity have been derived semi-classically as well as in the framework of quantum electrodynamics (Haroche 1976). The result can be written in the form

$$I(t) \propto \mathrm{Tr}_e\{\rho_e(t)\mathscr{D}\} \tag{1}$$

where

$$\mathscr{D} = \sum_f (\boldsymbol{e}_d \cdot \boldsymbol{D})|f\rangle\langle f|(\boldsymbol{e}_d^* \cdot \boldsymbol{D}) \tag{2}$$

is the detection operator ($\boldsymbol{D}$ is proportional to the electric-dipole operator) and where $\rho_e(t)$, the excited-state density matrix, describes the evolution of the excited state after the pulse. A simple expression for $\rho_e(t)$ is obtained assuming that the following conditions are satisfied.

(i) The excitation is 'broadline': $\Delta \gg T^{-1}$, where Δ is the spectral width of the exciting light and T is the duration of the pulse.

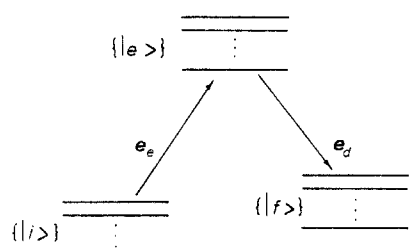

Figure 1. A typical quantum-beat experiment: energy levels and transitions involved.

(ii) The excitation is weakly coupled to the atomic system: $T \ll T_p$, the average time between two successive photon absorptions by an atom (conditions (i) and (ii) imply that, during the pulse, the probability per unit time for an atom to be excited is small compared to Δ: $\Delta \gg T_p^{-1}$).

(iii) The duration of the pulse is short compared to the characteristic times of the atoms: $T \ll \tau_e$, the common natural lifetime of the excited states, and for all e, e', $T \ll \omega_{ee'}^{-1}$ the Bohr frequencies corresponding to the excited-state energy differences.

Under these conditions $\rho_e(t)$ can be shown to be of the form

$$\langle e|\rho_e(t)|e'\rangle = \sum_{ii'} \langle e|\boldsymbol{e}_e \cdot \boldsymbol{D}|i\rangle \langle i|\rho_i(-T)|i'\rangle \langle i'|\boldsymbol{e}_e^* \cdot \boldsymbol{D}|e'\rangle \exp[-(\mathrm{i}\omega_{ee'} + \Gamma_e)t] \tag{3}$$

where $\rho_i(-T)$ is the density matrix of the initial state prior to the pulse. In this expression $\Gamma_e = \tau_e^{-1}$: the relaxation is assumed to be purely radiative. Substitution of (3) and (2) in (1) then leads to the following result for the intensity of the fluorescent light detected:

$$I(t) \propto \sum_{\substack{f \\ ii' \\ ee'}} \langle e|\boldsymbol{e}_e \cdot \boldsymbol{D}|i\rangle \langle i|\rho_i(-T)|i'\rangle \langle i'|\boldsymbol{e}_e^* \cdot \boldsymbol{D}|e'\rangle \times \langle e'|\boldsymbol{e}_d \cdot \boldsymbol{D}|f\rangle \langle f|\boldsymbol{e}_d^* \cdot \boldsymbol{D}|e\rangle \exp[-(\mathrm{i}\omega_{ee'} + \Gamma_e)t]. \tag{4}$$

3. Hyperfine-structure quantum beats

In the following, attention will be centred on the case of hyperfine-structure quantum beats; the atoms are assumed to have a non-zero nuclear spin, their fine-structure energy levels being sufficiently separated to permit selective excitation of multiplet members. The atomic states will be represented by

$$|a\rangle \equiv |\alpha(J_a I)F_a M_a\rangle \equiv |F_a M_a\rangle \qquad (a = i, e, f) \tag{5}$$

where the labels have their usual meaning; J_a denotes the total electronic angular momentum, I the nuclear spin, F_a the total angular momentum and M_a the quantum number corresponding to its projection on the z axis. α stands for all other labels necessary to identify each state. For simplicity we will furthermore assume that the initial state is not polarised before the pulse (its density matrix is proportional to the unit matrix) and that, with the exception of the light, there are no external fields present. In that case equation (4) becomes

$$I(t) \propto \sum_{\substack{F_e M_e \\ F_e' M_e' \\ F_i M_i \\ F_f M_f}} \langle F_e M_e|\boldsymbol{e}_e \cdot \boldsymbol{D}|F_i M_i\rangle \langle F_i M_i|\boldsymbol{e}_e^* \cdot \boldsymbol{D}|F_e' M_e'\rangle \times \langle F_e' M_e'|\boldsymbol{e}_d \cdot \boldsymbol{D}|F_f M_f\rangle \langle F_f M_f|\boldsymbol{e}_d^* \cdot \boldsymbol{D}|F_e M_e\rangle \exp[-(\mathrm{i}\omega_{F_e F_e'} + \Gamma_e)t]. \tag{6}$$

This equation is quite general but affords little direct insight into the phenomena. A better understanding of the quantum-beat lineshapes may be gained by eliminating all irrelevant quantum numbers, thus making the dependence on the characteristics of the atoms and of the excitation-detection process more explicit. In order to achieve this, two properties of equation (6) must be noted.

(i) The expression is clearly invariant under rotations and it should therefore be possible to eliminate the explicit dependence on the M_F quantum numbers.

(ii) The equation is independent of the level splittings in the initial and final states, allowing the summations over F_i, F_f to be carried out.

The first step of the calculation consists in reducing the electric-dipole matrix elements, making explicit their M_F dependence by using the Wigner–Eckart theorem and their F dependence by using the well known reduction formulae (Brink and Satchler 1971, p 152). This yields the following result:

$$I(t) \propto \sum_{\substack{F_eF'_e \\ pp' \\ p_0p'_0 \\ F_iF_f}} (-1)^{p_0+p'_0+p+p'+F_e+F'_e+F_i+F_f}(2J_e+1)^2(2F_e+1)(2F'_e+1)(2F_i+1)(2F_f+1)$$
$$\times (e_e)_{-p_0}(e^*_e)_{-p'_0}(e_d)_{-p}(e^*_d)_{-p'} \exp[-(i\omega_{F_eF'_e}+\Gamma_e)t]$$
$$\times |\langle J_e\|\boldsymbol{D}\|J_i\rangle|^2|\langle J_e\|\boldsymbol{D}\|J_f\rangle|^2 \begin{Bmatrix} F_e & F_i & 1 \\ J_i & J_e & I \end{Bmatrix}\begin{Bmatrix} F_i & F'_e & 1 \\ J_e & J_i & I \end{Bmatrix}$$
$$\times \begin{Bmatrix} F'_e & F_f & 1 \\ J_f & J_e & I \end{Bmatrix}\begin{Bmatrix} F_f & F_e & 1 \\ J_e & J_f & I \end{Bmatrix} X(F_e, F'_e, F_i, F_f; p_0, p'_0, p, p') \tag{7}$$

where

$$X(F_e, F'_e, F_i, F_f; p_0, p'_0, p, p')$$
$$= \sum_{\substack{M_eM'_e \\ M_iM_f}} (-1)^{F_e-M_e+F'_e-M'_e+F_i-M_i+F_f-M_f}$$
$$\times \begin{pmatrix} F_e & 1 & F_i \\ -M_e & p_0 & M_i \end{pmatrix}\begin{pmatrix} F_i & 1 & F'_e \\ -M_i & p'_0 & M'_e \end{pmatrix}\begin{pmatrix} F'_e & 1 & F_f \\ -M'_e & p & M_f \end{pmatrix}\begin{pmatrix} F_f & 1 & F_e \\ -M_f & p' & M_e \end{pmatrix} \tag{8}$$

and where the e_μ are spherical components of the polarisation vectors. Expression (8) can be readily evaluated using the graphical methods of angular-momentum theory (Brink and Satchler 1971):

$X(F_e, F'_e, F_i, F_f; p_0, p'_0, p, p')$

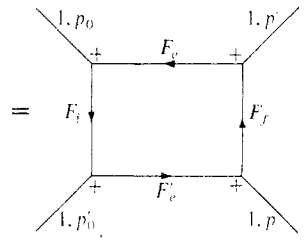

$$= \sum_k (2k+1) \cdot$$

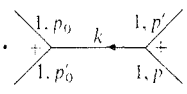

$\cdot$

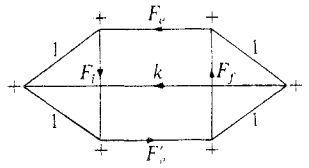

$$= \sum_k (2k+1) \cdot$$

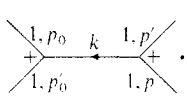

$\cdot$

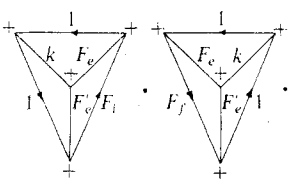

$\cdot (-1)^{k+2F_f-F_e-F'_e}$

$$= \sum_{kq} (-1)^{q+2F_f-F_e-F'_e}(2k+1)\begin{pmatrix} 1 & 1 & k \\ p_0 & p'_0 & q \end{pmatrix}\begin{pmatrix} 1 & 1 & k \\ p & p' & -q \end{pmatrix} \times \begin{Bmatrix} F_i & F_e & 1 \\ k & 1 & F'_e \end{Bmatrix}\begin{Bmatrix} 1 & k & 1 \\ F_e & F_f & F'_e \end{Bmatrix}. \tag{9}$$

Substitution of (9) in (7) gives, after some rearranging,

$$I(t) \propto \sum_{\substack{p_0 p'_0 \\ p p' \\ F_e F'_e \\ kq}} (-1)^{q-J_i+J_f}(2k+1)(2F_e+1)(2F'_e+1)(2J_e+1)^2 |\langle J_e\|\boldsymbol{D}\|J_i\rangle|^2 |\langle J_e\|\boldsymbol{D}\|J_f\rangle|^2 \times \exp[-(i\omega_{F_eF'_e}+\Gamma_e)t](e_e)_{-p_0}(e_e^*)_{-p'_0}(e_d)_{-p}(e_d^*)_{-p'} \times \begin{pmatrix} 1 & 1 & k \\ p_0 & p'_0 & q \end{pmatrix}\begin{pmatrix} 1 & 1 & k \\ p & p' & -q \end{pmatrix} Y(F_e, F'_e; k) Z(F_e, F'_e; k) \tag{10}$$

with

$$Y(F_e, F'_e; k) = \sum_{F_i} (2F_i+1)(-1)^{2J_e+k+F_e+F'_e+I+J_i+F_i} \times \begin{Bmatrix} F_e & F_i & 1 \\ J_i & J_e & I \end{Bmatrix}\begin{Bmatrix} F'_e & F_i & 1 \\ 1 & k & F_e \end{Bmatrix}\begin{Bmatrix} I & F_i & J_i \\ 1 & J_e & F'_e \end{Bmatrix} \tag{11}$$

and

$$Z(F_e, F'_e; k) = \sum_{F_f} (2F_f+1)(-1)^{2J_e+k+F_e+F'_e+I+J_f+F_f} \times \begin{Bmatrix} F'_e & F_f & 1 \\ J_f & J_e & I \end{Bmatrix}\begin{Bmatrix} F_e & F_f & 1 \\ 1 & k & F'_e \end{Bmatrix}\begin{Bmatrix} I & F_f & J_f \\ 1 & J_e & F_e \end{Bmatrix}. \tag{12}$$

The contractions in (11) and (12) can again be carried out in a straightforward manner using the graphical methods. For $Y(F_e, F'_e; k)$, for instance, one finds:

$$Y(F_e, F'_e; k) = \sum_{F_i} (2F_i+1) \cdot$$

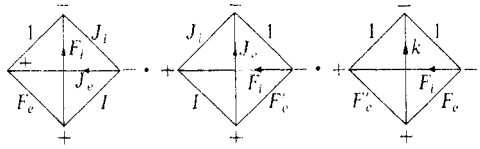

$$=$$

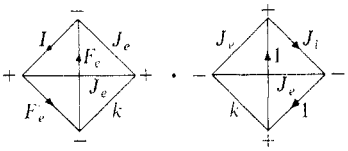

$$= \begin{Bmatrix} k & J_e & J_e \\ I & F_e & F'_e \end{Bmatrix}\begin{Bmatrix} k & J_e & J_e \\ J_i & 1 & 1 \end{Bmatrix}. \tag{13}$$

Introducing (13) and the analogous result for $Z(F_e, F'_e; k)$ into (10), one obtains the following final expression for the observed fluorescence intensity:

$$I(t) \propto (2J_e+1)^2(-1)^{J_i-J_f}|\langle J_e\|\boldsymbol{D}\|J_i\rangle|^2 |\langle J_e\|\boldsymbol{D}\|J_f\rangle|^2 \times \sum_{\substack{kq \\ F_e F'_e}} (-1)^q E^k_q U^k_{-q} A^k(F_e F'_e) B^k(F'_e F_e) \exp[-(i\omega_{F_eF'_e}+\Gamma_e)t] \tag{14}$$

where

$$E^k_q = \sqrt{2k+1}\sum_{p_0 p'_0}\begin{pmatrix}1 & 1 & k\\ p_0 & p'_0 & q\end{pmatrix}(e_e)_{-p_0}(e^*_e)_{-p'_0} \tag{15}$$

$$U^k_{-q} = \sqrt{2k+1}\sum_{pp'}\begin{pmatrix}1 & 1 & k\\ p & p' & -q\end{pmatrix}(e_d)_{-p}(e^*_d)_{-p'} \tag{16}$$

$$A^k(F_eF'_e) = [(2F_e+1)(2F'_e+1)]^{1/2}\begin{Bmatrix}F_e & F'_e & k\\ J_e & J_e & I\end{Bmatrix}\begin{Bmatrix}1 & 1 & k\\ J_e & J_e & J_i\end{Bmatrix} \tag{17}$$

$$B^k(F'_eF_e) = [(2F_e+1)(2F'_e+1)]^{1/2}\begin{Bmatrix}F'_e & F_e & k\\ J_e & J_e & I\end{Bmatrix}\begin{Bmatrix}1 & 1 & k\\ J_e & J_e & J_f\end{Bmatrix}. \tag{18}$$

In expression (14) all irrelevant quantum numbers have been eliminated, while the electric-dipole matrix elements have been broken up into factors with a clear physical meaning. The factor $|\langle J_e\|\boldsymbol{D}\|J_i\rangle\langle J_e\|\boldsymbol{D}\|J_f\rangle|^2$, containing the reduced matrix elements, is angle independent and describes the strength of the $J_i \rightarrow J_e$ and $J_e \rightarrow J_f$ transitions. Since it does not depend on the F quantum numbers, it does not affect the lineshape. The factors E^k_q and U^k_{-q} are purely angular, representing the polarisation characteristics of excitation and detection. $A^k(F_eF'_e)$ and $B^k(F'_eF_e)$ depend on the atomic quantum numbers and express the angular properties of the transitions involved. Again, their evaluation is straightforward. The last factor describes the time dependence of the different quantum-beat components.

4. Discussion

A few remarks must be made on the way this expression, which is nothing but an expansion of equation (6) in multipoles, was obtained. The multipoles were introduced quite naturally by applying the graphical method to the reduction of expression X; expanding in multipoles corresponds to a transformation of the type

$$\underline{a\alpha \qquad a\alpha'}\quad \underline{b\beta \qquad b\beta'} = \sum_k (2k+1)\,. \tag{19}$$

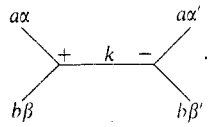

From the graphs it is clear that the procedure followed in order to obtain (9) is not unique. Another way of transforming the graph representing X is, for instance,

$X(F_e, F'_e, F_i, F_f; p_0, p'_0, p, p')$ =

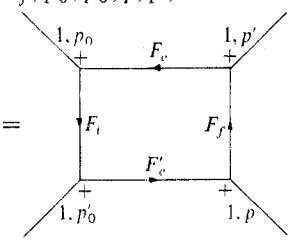

$= \sum_k (2k+1)$.

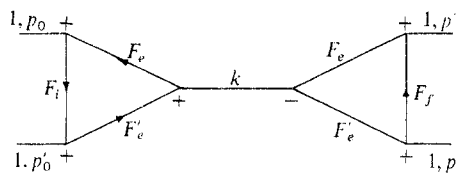

$$= \sum_k (2k+1) \cdot$$

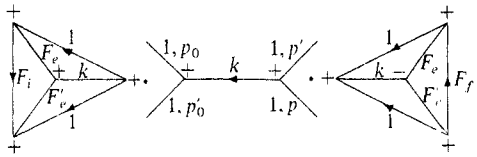

leading to the same result (9).

In the first case the k, q result from the coupling of two angular momenta 1 describing the light fields, in the second they result from the coupling of the atomic angular momenta. That in both cases the same simple result

$$k = 0, 1, 2$$

(corresponding to population, orientation and alignment, respectively) is found, derives from the fact that by optical means no multipoles of higher order can be induced or detected (photons being spin-1 systems).

In fact, the second reduction corresponds to the usual procedure followed to obtain the multipole expansion, i.e. by the introduction of irreducible spherical tensor operators

$$T^k_q(F_e F'_e) = \sqrt{2k+1} \sum_{M_e M'_e} |F_e M_e\rangle\langle F'_e M'_e| (-1)^{F_e - M_e} \begin{pmatrix} F_e & k & F'_e \\ -M_e & q & M'_e \end{pmatrix}. \tag{20}$$

Calculations along those lines have been performed by Luypaert (1976) and yield identical results.

The properties of the different multipole contributions can easily be derived by inspection of expressions (14)–(18). The triangular conditions for the 6-j symbols show, for instance, which coherences correspond to each multipole; terms with a given k (0, 1 or 2) can contain only contributions from coherences between excited states with $\Delta F_e \leqslant k$. In particular, for $k = 0$ this implies $F_e = F'_e$, so that the population contribution to the signal is always unmodulated.

As will be shown in the next section, terms with $k = 0, 1, 2$ can arise in experiments making use of circular polarisers, while in experiments using linear polarisers $k = 1$ contributions are excluded.

5. Examples

Although expression (14) has a rather complicated appearance, it is easily applicable to practical experimental arrangements. This will be illustrated here in two particular cases.

5.1. *Plane-polarised excitation and detection*

The first experimental geometry considered, involving plane polarisers, is shown in figure 2. The laboratory z axis is chosen to coincide with the direction of the detection polarisation e_d, while the direction of the excitation polarisation e_e is defined by the polar angles θ and ϕ. In this case the detection-polarisation dependent factor in equation (14) takes the form

$$U^k_{-q} = \sqrt{2k+1}\, \delta_{q0} \begin{pmatrix} 1 & 1 & k \\ 0 & 0 & 0 \end{pmatrix}. \tag{21}$$

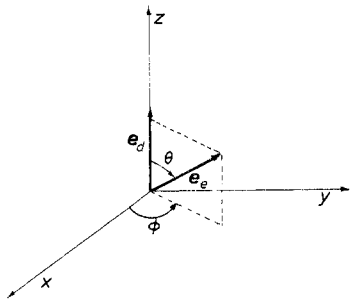

Figure 2. Excitation-detection geometry using linear polarisers.

The corresponding quantity characterising the exciting light can be obtained by first deriving its expression in a reference frame x'', y'', z'' making Euler angles $(0, -\theta, -\phi)$ with the lab frame. In this frame the excitation polarisation is parallel to the z'' axis and therefore $(E^k_q)'' = U^k_{-q}$. Transforming back to the lab frame and noting that $U^k_{-q} = 0$ unless $q = 0$, one finds that the only terms in (14) which do not vanish are those containing the factors

$$E^k_0 U^k_0 = (2k + 1)\begin{pmatrix} 1 & 1 & k \\ 0 & 0 & 0 \end{pmatrix} \mathscr{R}^k_{00}(0, \theta, \phi) \tag{22}$$

with $k = 0, 2$. The $\mathscr{R}^k_{00}(0, \theta, \phi)$ are rotation matrix elements, given by

$$\mathscr{R}^k_{00}(0, \theta, \phi) = P_k(\cos\theta), \tag{23}$$

the Legendre polynomials. From these expressions one can conclude:

(i) no orientation ($k = 1$) can be induced or detected using linear polarisers;

(ii) the population terms ($k = 0$) are angle independent;

(iii) the angular dependence for the alignment is as $(3\cos^2\theta - 1)$, which means there exists an angle between the two polarisers ($\theta = 54{\cdot}7°$) for which no alignment effects will be observed.

5.2. *Circularly polarised excitation and detection*

A second interesting experimental configuration is outlined in figure 3. The laboratory z axis is chosen to be parallel to the direction of observation, while the direction of the exciting beam is defined in the (yz) plane by the angle Θ it makes with the

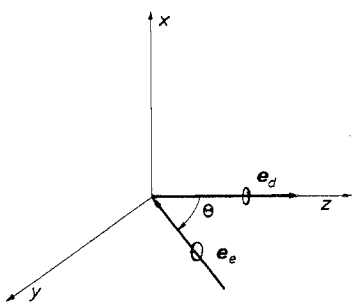

Figure 3. Excitation-detection geometry using circular polarisers.

z axis. A derivation along the same lines as in the previous case now yields only non-vanishing contributions with

$$E_0^k U_0^k = (2k+1)\begin{pmatrix} 1 & 1 & k \\ -1 & 1 & 0 \end{pmatrix}^2 P_k(\cos\Theta) \tag{24}$$

leading to the following conclusions.

(i) In addition to population and alignment terms, one can now have orientation terms.

(ii) The angular dependence of the terms with $k = 1$ is of the type $\cos\Theta$, implying that orientation effects cannot be observed for $\Theta = 90°$. This is an important result in connection with the study of hyperfine structures in $J = \frac{1}{2}$ states, in which only orientation effects can occur.

In figure 4 the validity of (14) is tested against an experimental result for hyperfine-structure beats from the $9^2D_{3/2}$ state of ^{133}Cs (I_π: polarisers parallel). Comparison of the experimental and theoretical lineshapes shows excellent agreement. (Details about the experiment can be found in the paper by Deech *et al* (1975).)

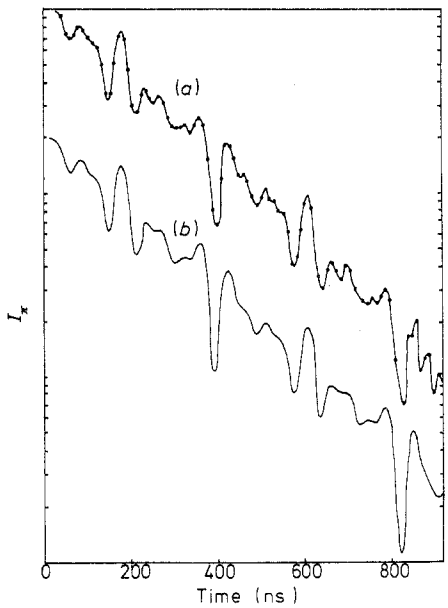

Figure 4. (*a*) Experimental decay spectrum for $9^2D_{3/2}$: I_π (logarithmic scale) against time. The full curve has been drawn to join the experimental points with no attempt to smooth statistical fluctuations (Deech *et al* 1975). (*b*) Theoretical curve calculated from equation (14).

6. Conclusion

By the introduction of multipoles, a well known procedure in optical-pumping theory, it is possible to obtain a clear physical understanding of experimental lineshapes. In this article the technique has been applied to the discussion of hyperfine-structure quantum beats. It was noted that the calculations are considerably simplified by the use of the graphical methods of angular-momentum theory; there is no need for

introducing explicit expressions for irreducible spherical tensors, while all contractions are carried out automatically in the course of transforming graphs. The final expression for the lineshape was cast in a form, well adapted to applications, separating factors pertaining to the atomic system from those relating to the excitation-detection scheme.

References

Aleksandrov E B 1963 *Opt. Spectrosc.* **14** 233
——1964 *Opt. Spectrosc.* **17** 252
Andrä H J 1970 *Phys. Rev. Lett.* **25** 325
Brink D M and Satchler G R 1971 *Angular Momentum* 2nd edn (Oxford: Clarendon)
Colegrove F D, Franken P A, Lewis R R and Sands R H 1959 *Phys. Rev. Lett.* **3** 420
Corney A and Series G W 1964 *Proc. Phys. Soc.* **83** 207
Deech J S, Luypaert R and Series G W 1975 *J. Phys. B: Atom. Molec. Phys.* **8** 1406
Dodd J N, Sandle W J and Zissermann D 1964 *Proc. Phys. Soc.* **92** 497
Hadeishi T and Nierenberg W A 1965 *Phys. Rev. Lett.* **14** 891
Hanle W 1924 *Z. Phys.* **30** 93
Haroche S 1976 *Topics in Applied Physics, vol 13, High Resolution Laser Spectroscopy* ed K Shimoda (Berlin: Springer Verlag)
Haroche S, Paisner J A and Schawlow A L 1973 *Phys. Rev. Lett.* **30** 948
Luypaert R 1976 *PhD Thesis* University of Reading